ELSEVIER

Polymer 40 (1999) 3909–3918

polymer

Stress relaxation of polypropylene fibres with various morphologies

Erik Andreassen*

SINTEF, P.O. Box 124 Blindern, N-0314 Oslo, Norway

Received 27 May 1998; received in revised form 23 July 1998; accepted 20 August 1998

Abstract

Melt-spun polypropylene fibres with various molecular weight distributions (MWDs) and processing parameters were subjected to stress relaxation tests at 23 and 100°C. The average level of the relaxation curves was mainly determined by processing conditions, but the MWD affected the relaxation kinetics substantially, especially at 100°C. In general, the relaxation rate was reduced by increasing the molecular orientation, increasing the degree of crystallinity, and broadening the MWD. However, the effect of the MWD was reversed for the initial relaxation at 100°C. MWD effects at 23 and 100°C were in accordance with relaxation spectra obtained by dynamic mechanical analysis. Stress plateaus at long relaxation times were observed for broad MWDs at 100°C. The presence of a crystalline structure seems to be a prerequisite for both the 'reversed' MWD effect and the stress plateaus. The observations reported in this study can be interpreted in terms of molecular reptation, molecular constraints and structural relaxation.

Keywords: Polypropylene; Fibres; Stress relaxation

1. Introduction

Most of the earlier studies on the viscoelastic properties of polypropylene (PP) only considered one single sample, while applying a wide range of analysis parameters (temperatures, deformation rates, etc.). However, the viscoelastic response may be substantially influenced by material parameters and processing conditions. This article describes some of these effects.

Solid-state rheometry provides information on the kinetics of relaxation mechanisms, i.e. the viscoelastic behaviour [1]. Measurements of this kind may be a part of fundamental studies, or they are applied directly when evaluating materials and processes for commercial products. Creep (constant stress) and stress relaxation (constant strain) tests are perhaps the simplest techniques for analyzing the relaxation of polymeric structures.

Many early publications on stress relaxation dealt with amorphous materials, and the behaviour of these single-phase materials is fairly well understood [2,3]. The viscoelastic response of semi-crystalline materials, such as PP, is more complex [4,5]. A number of fundamental studies on the mechanical relaxations in PP have been published [4,6–10], dealing with molecular mechanisms and kinetics. Recent studies on stress relaxation in PP have focused on time–temperature superposition (master curves) [11–13], non-linear effects [14,15], viscoelastic constitutive equations [16], effects of strain rate and cyclic preloading [17–20], blends [21], and the interaction between viscoelastic and structural relaxation [22]. One type of structural relaxation that has received much attention is physical ageing. Creep measurements have been used in many of these studies on PP [23–27], but stress relaxation tests have been applied as well [28]. Internal stresses have also been considered in relation to the viscoelasticity of PP [29].

The literature on morphological effects—via molecular parameters and/or processing conditions—is sparse. Attalla et al. [30] prepared a set of compression moulded samples with large variations in crystallinity and spherulite size (only one PP grade was used). The stress relaxation was measured at temperatures from −20 to 40°C. Master curves were obtained for each sample. The relaxation spectra were affected by morphology in a complex way, and no simple method could be found to correlate the various master curves. Passaglia and Martin [31] studied a similar set of PP samples by dynamic mechanical thermal analysis (DMTA). All the relaxation peaks changed in intensity and position as a function of morphological parameters. They also found that the loss modulus and the loss compliance changed in different ways. Hence, the outcome of a comparison between different samples would depend on whether the comparison was made at equivalent strains or stresses. This was attributed to the microscopic connectivity of crystalline and amorphous phases. Kawamoto et al. [32]

* *E-mail address:* Erik.Andreassen@matek.sintef.no (E. Andreassen)

0032-3861/99/$ - see front matter
PII: S0032-3861(98)00622-3

Table 1
Material parameters and processing conditions for the six fibres considered in this study

Sample code[a]	M_w/M_n	Melt index[b]	Draw-down ratio[c]	Draw ratio[d]
NH	~3	25	77	3
BH	~5	20	77	3
NL	~3	25	155	1.5
BL	~5	20	155	1.5
NA	~3	25	38	–
BA	~5	20	38	–

[a] B, broad MWD; N, narrow MWD; H, high draw ratio; L, low draw ratio; A, as-spun.
[b] ISO 1133 (g per 10 min).
[c] The ratio of spinning speed to extrusion speed. The extrusion temperature was 280°C for most of the fibres. The cooling air speed was set very low for the two as-spun fibres, in order to obtain a mesomorphic structure.
[d] The temperature of the drawing chamber was 165°C.

recently analyzed PP samples varying in surface crystallinity in a similar fashion. By applying the Takayanagi model, the results were attributed to differences between the bulk and the surface regarding the continuity of the amorphous phase. Crissman [33] reported effects on the DMTA curves due to the composition of crystallographic phases (α and β phases of isotactic PP), and the orientation of lamellae. There are many reports on orientation effects in PP using DMTA [34–36], and one main observation is that the intensity of the β relaxation (glass transition) decreases with increasing orientation. This has been attributed to taut tie-molecules and compressed interfibrillar amorphous layers [34]. Hadley and Ward [37] applied the multiple integration representation to creep and recovery data of PP fibres, and found that non-linear effects could be described by a few terms in this representation. These terms changed in a consistent manner with changes in morphology, and molecular orientation was the main morphological parameter.

When it comes to material parameters of PP in relation to mechanical relaxations, there are a few studies on blends, copolymers and tacticity parameters [21,38]. Furthermore, Hadley and Ward [37] reported that fibres with different molecular weights had similar creep and recovery data, but the compliance level decreased with increasing molecular weight. The author is not aware of any study focusing on the molecular weight distribution (MWD) in relation to mechanical relaxations. Effects of the MWD on the relaxation spectra of PP melts have, however, been reported [39]. All the studies referred to above used isotactic PP. Mechanical relaxations in syndiotactic PP were considered recently [40].

The present article describes how the interaction between MWD and processing conditions for melt-spun fibres influences the stress relaxation. Substantial effects of this interaction on various mechanical properties were observed in previous studies [41,42]. The fibres examined represent a wide range of morphologies, in terms of molecular orientation (high/low and uniaxial/bimodal), order (mesomorphic/α phase) and density. Previous studies by the present author and coworkers, involving similar fibre sets, focused on structure development and mechanical properties [41,43], simulation of the spinning stage [44], internal stresses [45], melting behaviour [46], non-woven fabrics [47], and models for the tensile deformation of various fibre assemblies [42].

2. Experimental

The fibres were produced in a full-scale spinning line, consisting of three integrated stages: *spinning* (from melt), *drawing* (in the solid state) and *annealing*. This spinning line, and the resulting structures and properties of the fibres, were presented in earlier papers (see Ref. [41]).

Six different fibres were analyzed in this study, representing the combinations of two MWDs (narrow and broad) and three processing categories (as-spun, low draw ratio and high draw ratio) (see Table 1). All the materials are isotactic homopolymers. The narrow MWD was produced by peroxide degradation. There are some minor differences between the processing parameters of the two samples in each processing category, i.e. the difference between the fibres 'Nx' and 'Bx' (x = A, H and L) has a minor component due to processing. However, the major effects of MWD and processing conditions on the relaxation curves are well probed in this study.

The relaxation of tensile stress was recorded at 23 and 100°C. The two fibres processed with a high draw ratio (NH and BH) were also tested at 65°C and 135°C. The strain was 1.8% in all experiments. This relatively high strain value was selected in order to obtain a sufficient signal with as-spun fibres at 100°C. (Wortmann and Schultz [15] reported linear viscoelastic behaviour of their PP samples for strains up to 1%. Dutta and Edward [16] found that the strain at 30°C had to be below 0.3% in order to be in the linear regime. However, they found no substantial change in the shape of the relaxation curve for strains up to 4%.) The sample length between the clamps was approximately 25 mm. The stress relaxation was recorded for 3 h with a Rheometrics RSA-II instrument. This instrument controls the separation of the clamps and measures the force. Hence, it is well suited for stress relaxation experiments. A constant strain level was reached in less than 0.05 s, and reliable data for the relaxation moduli, $E(t)$, were obtained after ~0.05 s.

Single fibres were tested at low temperatures, while small fibre bundles had to be used at high temperatures (for all six fibre types). There will always be some slack in a bundle. Hence, compared to a single fibre, a bundle will have lower effective modulus and a somewhat modified stress–strain response. However, these experimental errors have no significant effect on the main observations in this study.

All fibres expanded somewhat when heated to 65°C.

Table 2
Selected fibre properties

Sample	Structure[a]	Orientation[a]	Density ($kg\ m^{-3}$)	Diameter (μm)	Tensile modulus ($\epsilon = 1\%$) (GPa)	Relative shrinkage[b] (23–100°C)
NH	α phase	High, unimodal	897	24	6.2	0.03
BH	α phase	High, unimodal	895	24	6.1	0.02
NL	α phase	Medium, slightly bimodal	895	24	4.0	0.005
BL	α phase	Medium, bimodal	900	24	4.2	0.01
NA	Mesomorphic	Almost isotropic	887	65	0.9	−0.04
BA	Mesomorphic	Almost isotropic	888	65	0.8	−0.04

[a] Based on wide-angle X-ray scattering and infrared dichroism data. In the literature on PP, the mesomorphic structure has also been referred to as smectic or paracrystalline.

[b] Estimated from the adjustment of the clamping length that was necessary in order to maintain a constant small pre-tension during heating. The shrinkage values were obtained after 15 min of thermal and structural equilibration at 100°C.

Drawn fibres started shrinking at higher temperatures, while as-spun fibres expanded further (see Table 2). The fibres were conditioned for 15 min prior to testing at temperatures above 23°C. During this period, the distance between the clamps was continuously adjusted in order to maintain a small constant pre-tension (the change in stiffness with increasing temperature was not compensated for).

About 15 parallels were tested for each fibre type and temperature. A third-order polynomial in ln t was fitted to $E(t)$ data recorded in the interval 10^{-1} to 10^{4} s. The data sets were well fitted by this polynomial (correlation coefficients (r^2) above 0.999), and polynomials with higher order terms did not give significantly better fits. The curves shown in this paper are drawn using third-order polynomials, with average values (from the parallels) for the four coefficients. The various derivatives considered below were calculated analytically from the polynomials.

All six fibres were also characterized by DMTA, using the same Rheometrics RSA-II instrument. The temperature was increased from −90 to 155°C in steps of 4°C, and the tensile strain was oscillated with amplitude 0.5% and frequency 2 Hz.

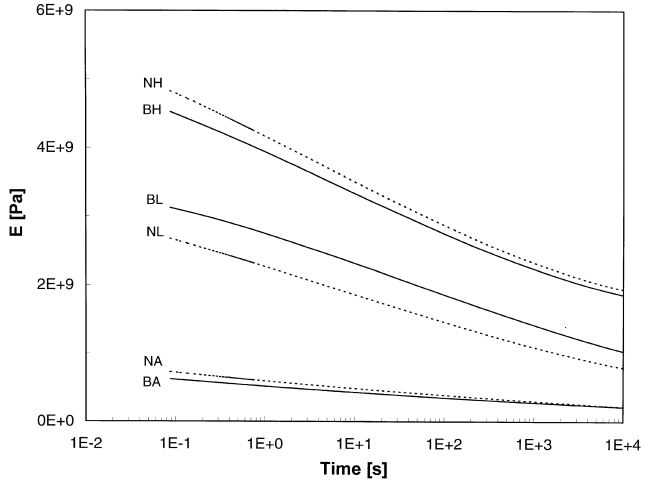

Fig. 1. Stress relaxation of various PP fibres at 23°C.

3. Results and discussion

3.1. Stress relaxation at 23°C

The relaxation moduli, $E(t)$, of the six PP fibres at 23°C are shown in Fig. 1. The main distinction between the curves is due to processing. The MWD is only a secondary effect. The sequence of decreasing relaxation moduli from sample NH to sample BA was expected from the tensile moduli shown in Table 2. At high draw ratios, the highest modulus is typically obtained with a narrow MWD, while the opposite is observed at low draw ratios. The former effect is due to a more effective deformation for the narrow MWD during the drawing stage, and the latter effect is due to flow-induced orientation which is more pronounced with the broad MWD, which includes a high-molecular-weight tail. These issues were discussed in Ref. [41].

When considering the fraction of stress relaxed after 3 h, the main distinction is between the highly drawn fibres and the rest (see Table 3). The low degree of relaxation in the fibres NH and BH is probably related to molecular constraints due to high molecular orientation.

As a secondary effect, the degree of relaxation seems to be related to the MWD. Fibres with a broad MWD tend to have a somewhat lower degree of relaxation. This could be explained by longer reptation times, as well as constraints formed during the solidification of the oriented melt. (This MWD effect is probably overshadowed by the high draw ratio for the NH/BH pair.)

The shape of the relaxation curve, i.e. the relaxation kinetics, can be analyzed by calculating the derivatives. The initial response (from $t \sim 0.1$ s) is highlighted when plotting $E''(t)$ versus $E'(t)$ as in Fig. 2(a). Values for initial relaxation rates are given in Table 3. Again, the primary and secondary effects of processing conditions and MWD, respectively, are observed.

Normalized initial relaxation rates (E'/E) are also given in Table 3. As a first approximation, the normalized initial rates should be the same for fibres with different degrees of orientation, but otherwise similar structural features. Hence, the initial value of E'/E should give an indication

Table 3
Relaxation data[a] obtained at 23°C

Sample	Relaxed fraction $(E_i - E_f)/E_i$	Initial relaxation rate E_i' (GPa s^{-1})	Norm. initial relaxation rate E_i'/E_i (s^{-1})	Final relaxation rate E_f' (kPa s^{-1})	Norm. final relax. rate E_f'/E_f (10^{-6}/s)
NH	0.60	2.5	0.53	13	6.7
BH	0.59	2.2	0.49	13	6.9
NL	0.70	1.6	0.60	11	14
BL	0.67	1.3	0.42	14	14
NA	0.70	0.57	0.80	3.6	17
BA	0.65	0.44	0.72	2.6	12

[a] $E_i \equiv E(t = 0.1\ s)$ and $E_f \equiv E(t = 10^4\ s)$.

of the molecular ability for relaxation, as determined by structural features. When considering the normalized initial relaxation rates, the processing trends are not so clear, but the as-spun fibres have the highest values. This was expected, because these mesomorphic fibres have less molecular constraints. The MWD effect is the same as for unnormalized relaxation rates.

The kinetics at the end of the relaxation experiment ($t \sim 10^4$ s) is illustrated by the log–log plot of E'' versus E' in Fig. 2(b). Relaxation rates at $t = 10^4$ s are shown in Table 3. The main distinction in this regime is between as-spun and drawn fibres. As for the initial response, the lowest relaxation rates are observed for as-spun fibres. The rates are lower by about the same factor as for the initial response, i.e. the lower rates of as-spun fibres are not due to these fibres having reached a 'terminal' stage (end of relaxation). Normalized relaxation rates, on the other hand, are lowest in highly drawn fibres. A possible MWD effect is only observed for as-spun fibres, for which the relaxation rates with and without normalization are higher with the narrow MWD.

It was mentioned above that, as a first approximation, the normalized initial relaxation rates should be the same for samples with different degrees of orientation, but otherwise similar structural features. What about the relaxation at the end of the experiment? As mentioned in the previous paragraph, highly drawn fibres have the lowest normalized relaxation rates at the end of the experiment, as was the case for the initial stage. As-spun (mesomorphic) and moderately drawn fibres, on the other hand, have roughly the same normalized relaxation rate (and degree of relaxation) at the end of the experiment—in contrast to the initial behaviour. This may be due to structural reorganization occurring mainly in the mesomorphic samples. Some other possible explanations are summarized in the following two paragraphs.

Long relaxation times correspond to high temperatures, and in this case the relaxation of a crystalline PP structure is dominated by the α process. However, this process is probably not active in the mesomorphic as-spun fibres (see Section 3.3). This could explain the apparently low E'/E at the end of the experiment, as compared to the (crystalline) moderately drawn fibres. Initial E'/E values at 100°C agree with this picture: the normalized rates of as-spun fibres are not substantially above those of the other four fibres, as was the case initially at 23°C.

Two remarks should be made regarding the comparison

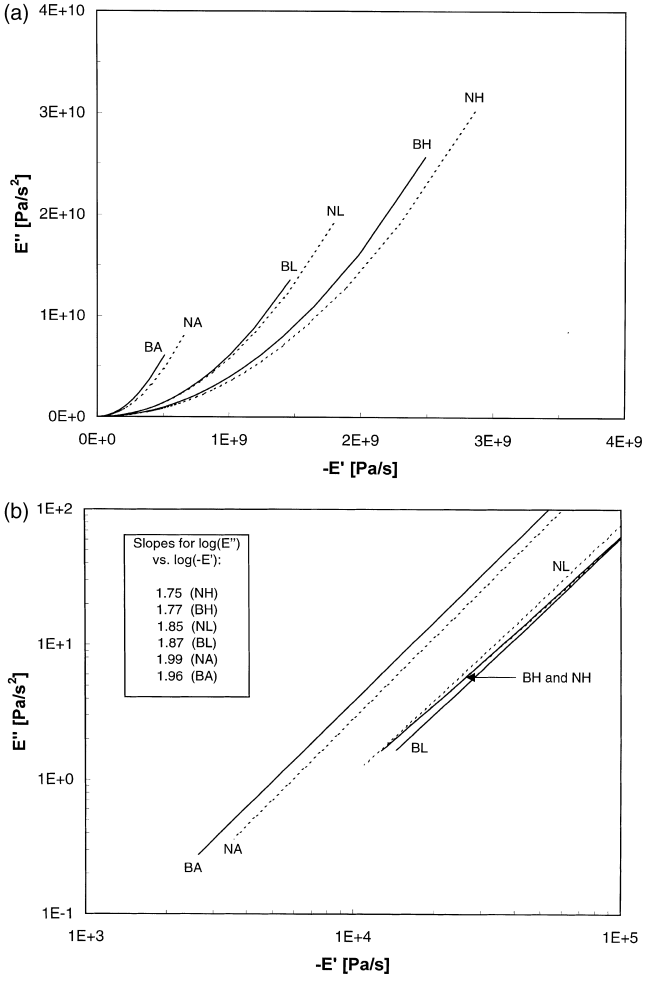

Fig. 2. $E''(t)$ versus $-E'(t)$ at 23°C in linear (a) and logarithmic (b) plots, describing the kinetics at the start and end of the experiment, respectively ($E' \equiv dE/dt$ etc.). The slopes reported in Fig. 2(b) are calculated from the curve segments contained within the figure.

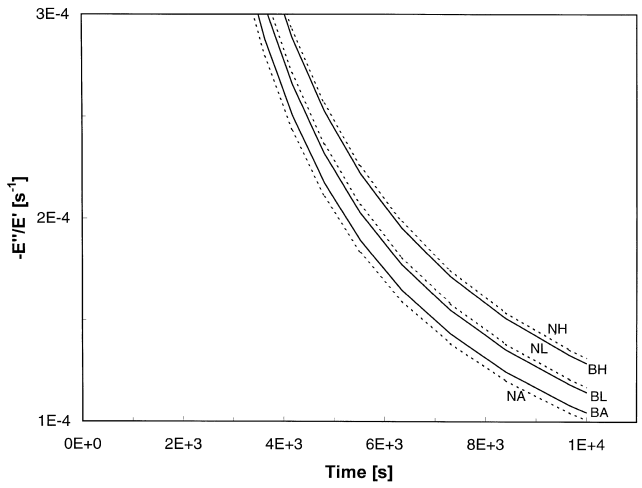

Fig. 3. $-E''/E'$ versus time at 23°C. Solid and dotted lines denote samples with broad and narrow MWDs, respectively.

of normalized relaxation rates: (1) a simple 'linear normalization', as applied here, may not be a relevant expression when comparing fibres after long relaxation times and at low stress levels; (2) at a molecular level, relaxation processes in crystalline polymers are often shear mechanisms [1], but tensile mechanisms have also been suggested [34]. The literature on this topic is sparse for PP, but there may be differences between crystalline and mesomorphic PP structures regarding shear versus tension; in particular since the α process is absent for the latter structure. Such differences would complicate the relationship between the degree of orientation and the relaxation rate (maximum shear occurs at an angle 45° to the loading direction). Hence, the normalized relaxation rates of different structures may not be fully comparable.

Fig. 2(b) shows that the ratio $\log(E'')/\log(-E')$ (at the end of the relaxation experiment) is related to processing conditions. This ratio decreases with increasing degree of orientation and crystallinity. An alternative plot is shown in Fig. 3, where E''/E' is plotted versus time. Note that these curves seem to obey a superposition principle. At the end of the relaxation experiment, the ratio E''/E' (or the logarithmic version mentioned earlier) distinguishes better between differently processed fibres than entities such as E', E'/E, E'' and E''/E.

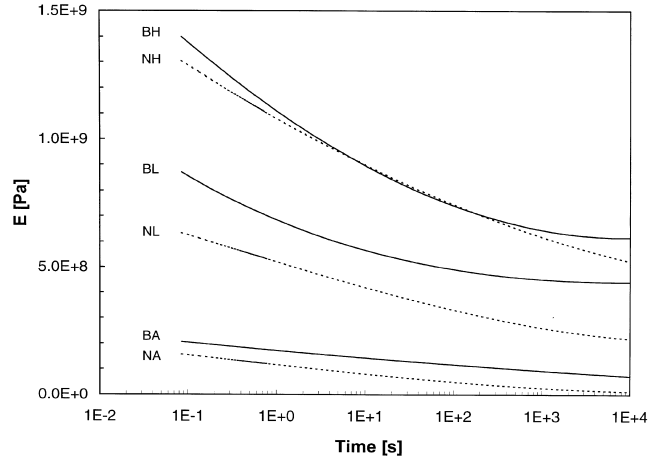

Fig. 4. Stress relaxation of various PP fibres at 100°C.

Finally, it should be noted that within a certain processing category there may be some interference between 'MWD effects' and 'modulus effects' (this issue was also mentioned in Section 2). However, there is not a one-to-one relationship between MWD and modulus. Hence, the MWD effects reported above seem to be correctly assigned.

3.2. Stress relaxation at 100°C

A number of MWD effects appear at this temperature, see Figs. 4 and 5 and Table 4. When comparing fibres with similar processing conditions, the relaxation curve of the fibre with the broad MWD is characterized by:

- a shift upwards in initial stress, i.e. the initial value of the difference $E(\mathrm{Bx}) - E(\mathrm{Nx})$ has increased and is positive for all pairs at this temperature;
- a higher initial relaxation rate; and
- a stress plateau at long relaxation times.

The two last effects only appear for drawn fibres. Another MWD effect is that the three fibres with narrow MWD have similar slopes in a log–log plot of E'' versus $-E'$, towards the end of the relaxation experiment (see Fig. 5(b)).

Various hypotheses may be considered for the effect of MWD on the initial response. The higher stiffness of fibres with a broad MWD could be due to higher structural integrity at this temperature, caused by the high-molecular-weight fraction. A similar effect is observed by DMTA (see Section 3.3). Furthermore, broad MWD fibres have a higher onset of melting, as measured by differential scanning calorimetry [46].

Drawn fibres with a narrow MWD have lower relaxation rates than fibres with a broad MWD at $t \sim 0.1$ s. The opposite effect, i.e. slower relaxation due to the longer molecules present in the broad MWD, is observed in most other cases. Fibres with a narrow MWD may already have experienced an early strong relaxation before entering the experimental window. However, there is no sign of this for the earliest obtainable data at $t \sim 0.04$ s. In fact, the trends seen in Fig. 4 go back to the earliest recordings. In data obtained at 65°C (corresponding to shorter relaxation times than the 100°C data), BH and NH have similar initial relaxation rates. The former has somewhat higher rates at intermediate times, but lower rates at long relaxation times (possibly a precursor to the plateau in Fig. 4).

At 100°C, one might suspect that differences observed in the early stage of relaxation may be due to shrinkage effects [22,34,48], i.e. different shrinkage forces. Although the fibres were conditioned for 15 min at 100°C, the shrinkage of drawn fibres had not stopped completely at the beginning

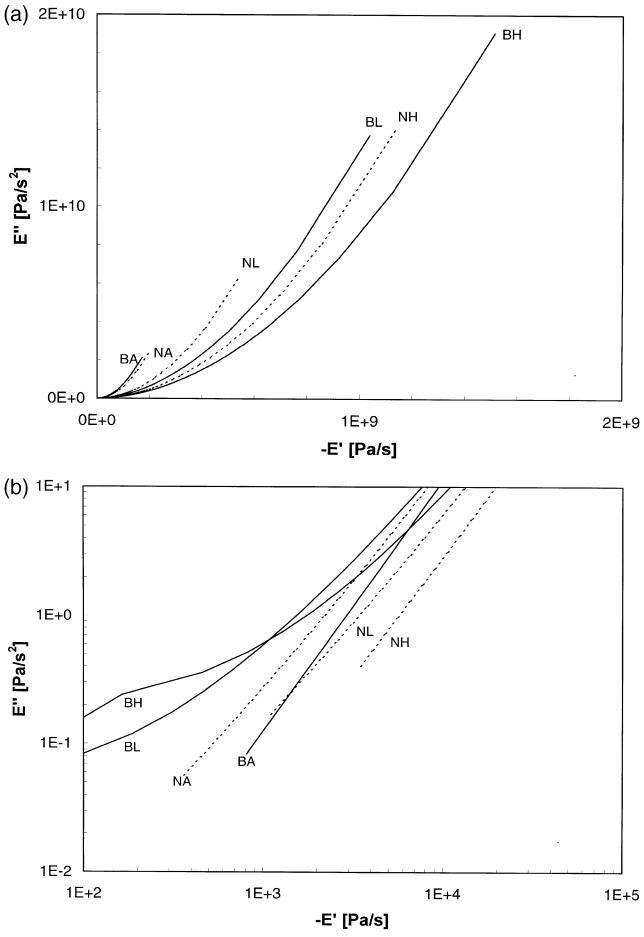

Fig. 5. $E''(t)$ versus $-E'(t)$ at 100°C in linear (a) and logarithmic (b) plots, describing the kinetics at the start and end of the experiment, respectively.

of the relaxation experiment. However, as shown in Table 2, there is no trend that fibre Nx shrinks more and faster than fibre Bx (x = H, L), which could result in an apparently slower initial relaxation for drawn fibres with a narrow MWD.

At long relaxation times, the MWD trend with regard to relaxation rates is reversed, and a stress plateau is reached for drawn fibres with a broad MWD. Since this effect is not observed with as-spun fibres, it must be due to a combination of MWD and structural characteristics. Row-nucleated crystallites, in particular, may provide 'anchorage' that hinders the relaxation.

'Entanglement' plateaus is a well known feature, especially for amorphous polymers [2,3]. Amorphous polymers is the best understood system in terms of stress relaxation, and 'stage 3' [2] of their relaxation consists of a plateau and a subsequent terminal zone, in which the stress drops sharply. The width and the stress of the plateau are related to molecular weight and degree of cross-linking [3] (if any). It has also been shown that the shape of the plateau is affected by the width of the MWD [3,49,50].

The plateaus in Fig. 4 may be attributed to physical crosslinks. However, other mechanisms than the pure relaxation of a linear viscoelastic material may be active. One indication for this is that the plateau of BH is absent at 135°C. At this temperature, NH and BH have roughly the same normalized relaxation rates at the end of the experiment ($\sim 2 \times 10^{-6}\ s^{-1}$, see Table 4 for comparisons).

Possible causes for the MWD effect in drawn fibres can be summarized as follows. The strong relaxation observed initially with the broad MWD may also be present for the narrow MWD, but shifted towards shorter times (lower temperatures). This relaxation mechanism may also be partially 'deactivated' for the narrow MWD, due to structural reorganization (annealing) (which may be easier with the narrow MWD). The stress plateau reached at long relaxation times with the broad MWD is probably due to physical crosslinks. Orientation-induced crystalline structures are likely to play a role in the formation of these constraints [5], but structural reorganization at elevated temperatures may also contribute.

The two as-spun fibres have about the same initial relaxation rate. At the end of the experiment, the fibre with the narrow MWD has the lowest rate, and its degree of relaxation is 92%, which is the highest value observed at this temperature. The relaxation rate of the fibre with broad MWD is twice as high at the same time, but its degree of relaxation is only 64%. In other words, the relaxation of this fibre seems to be delayed relative to the fibre with narrow MWD. This delay may be attributed to longer reptation times.

Table 4
Relaxation data[a] obtained at 100°C

Sample	Relaxed fraction $(E_i - E_f)/E_i$	Initial relaxation rate E_i' (GPa s^{-1})	Norm. initial relaxation rate E_i'/E_i (1 s^{-1})	Final relaxation rate E_f' (kPa s^{-1})	Norm. final relaxation rate E_f'/E_f (10^{-6} s^{-1})
NH	0.59	0.96	0.74	3.5	6.7
BH	0.55	1.3	0.92	$\sim 10^{-18}$	$\sim 10^{-18}$
NL	0.72	0.46	0.73	1.1	5.2
BL	0.48	0.86	1.0	$\sim 10^{-18}$	$\sim 10^{-18}$
NA	0.92	0.17	1.1	0.37	30
BA	0.64	0.15	0.72	0.84	11

[a] $E_i \equiv E(t = 0.1\ s)$ and $E_f \equiv E(t = 10^4\ s)$.

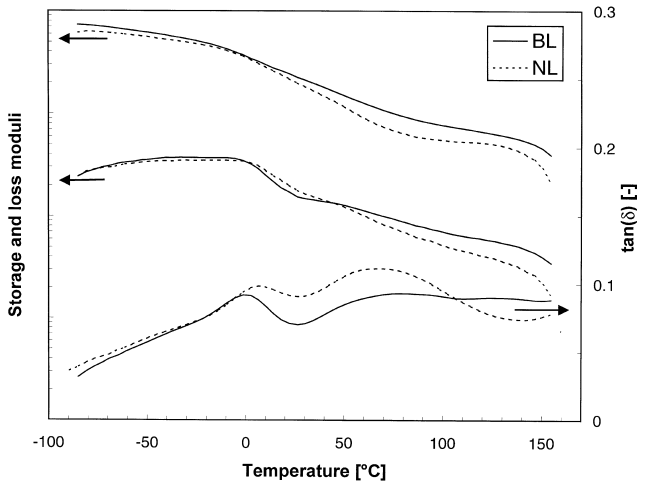

Fig. 6. DMTA data for the two moderately drawn fibres. Fibre bundles were tested, but the recorded storage (upper curves) and loss moduli were not normalized to the true cross-sectional area.

3.3. Relations between DMTA and stress relaxation data

DMTA curves provide details about the mechanical relaxations. Furthermore, the storage modulus versus temperature obtained by DMTA is related to the relaxation modulus versus time. The MWD effects presented in the preceding section can be clarified by considering the DMTA results.

The storage moduli of NL and BL are compared in Fig. 6. The former has the largest (negative) slope at 23°C, while the latter decreases fastest at 100°C. Both these observations agree with the stress relaxation experiments. An explanation for these effects is indicated by the tan(δ) curves in Fig. 6: NL has higher relaxation 'strength' than BL between the β relaxation (~0°C) and the high-temperature end of the α relaxation (~100°C). The 'terminal' plateau of BL, which was observed in Fig. 4, is not seen in Fig. 6. However, BL clearly has higher structural integrity than NL at high temperatures.

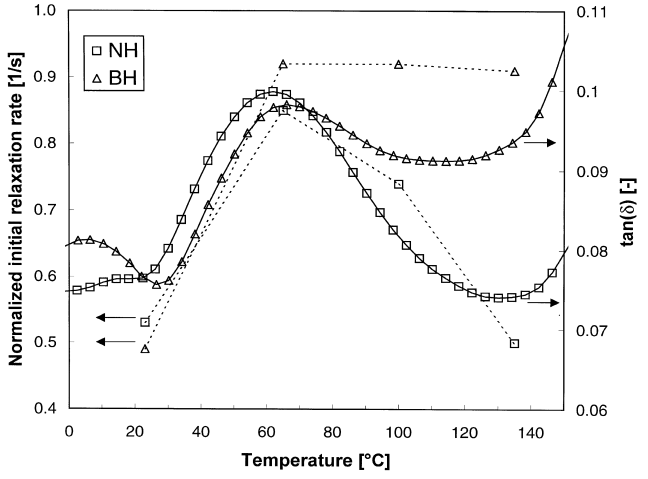

Fig. 7. Normalized initial relaxation rates and tan(δ) versus temperature for the two highly drawn fibres.

The normalized initial relaxation rates generally increase when going from 23 to 100°C (see Tables 3 and 4), i.e. the modulus is slightly more reduced than the relaxation rate. Some more details on this temperature effect are available for the highly drawn fibres, which were tested at four different temperatures. Normalized initial relaxation rates and tan(δ) values are shown together versus temperature in Fig. 7. As could be expected, there is a correlation between these initial relaxation rates and tan(δ).

The tan(δ) curves of all the six fibres are shown in Fig. 8. Note the good correlation between the tan(δ) values at 23°C and the corresponding normalized initial relaxation rates (Table 3). The most pronounced effect in Fig. 8 is that the β relaxation is reduced by the constraints on mobility caused by drawing, in agreement with earlier observations [34]. Also note the difference between drawn fibres with narrow and broad MWDs in the temperature interval 80–120°C: tan(δ) of the former decrease, while those of the latter are almost constant. The apparent peak observed for the as-spun fibres around 95°C is associated with the onset of melting, and it is not the α relaxation (which requires the presence of a crystalline phase). For all three pairs of narrow and broad MWDs, the narrow MWD gives higher tan(δ) values in an intermediate temperature range.

3.4. Kubát coefficients

Kubát et al. [51, 52] showed that the relation

$$\left(\frac{\mathrm{d}E}{\mathrm{d}(\ln t)}\right)_{\max} = \left(t\frac{\mathrm{d}E}{\mathrm{d}t}\right)_{\max} = K(E_\infty - E_0) \tag{1}$$

is valid for the stress relaxation of a wide range of materials, with $K \approx 0.1$. The two relaxation moduli at the right-hand side are the terminal and initial values, respectively. The significance of the Kubát coefficient, K, can be illustrated by considering the stretched exponential function,

$$E = E_0 \exp[-(t/\tau)^\gamma] \tag{2}$$

for which $K = \gamma/e$. Hence, K is a measure of the narrowness of the distribution. The most simple model for stress relaxation, the Maxwell model, has $\gamma = 1$, i.e. $K = 1/e \approx 0.37$. Eq. (2), also called the Kohlrausch–Williams–Watts (KWW) function, has been applied to many materials, and describes the initial stage of relaxation well. Real systems have broader distributions than the Maxwell model. A γ value near 1/2 is often measured for the 'stage 1' (segmental) relaxation of polymer liquids near equilibrium [2]. Below the glass transition temperature (non-equilibrium), γ drops to a lower value. For a wide range of materials, fits of the KWW function yields γ values between 1/4 and 1/3, in accordance with a Kubát parameter of 0.1 [53].

The left-hand side of Eq. (1) is plotted versus the relaxation modulus in Fig. 9. The curves of drawn fibres have maximum points. Extrapolation on the right-hand side of

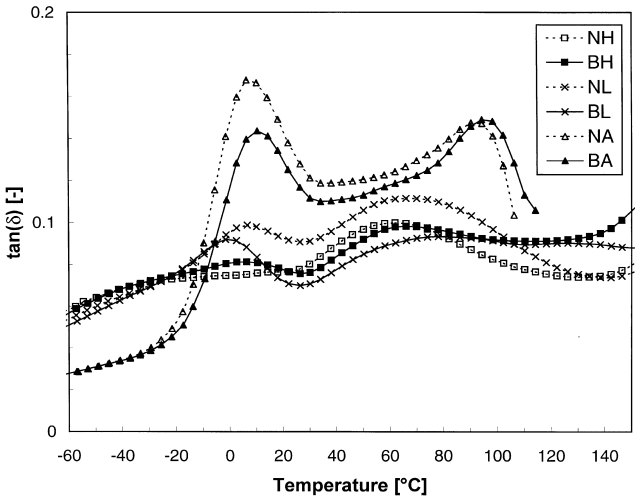

Fig. 8. tan(δ) curves for all six fibres considered in this study.

these maxima points towards $E(t = 0)$, and on the other side the terminal value $E(t \rightarrow \infty)$ (corresponding to zero relaxation rate) may be found. Extrapolations of this kind are, of course, dubious, especially since other relaxation mechanisms may be active outside the time scale of the experiment. However, some trends are illustrated by Fig. 9. In the limit $t \rightarrow \infty$, the asymptotic moduli of moderately drawn fibres are in the range 0–0.5 GPa. The highly drawn fibres, on the other hand, have asymptotic moduli in the range 1.5–2.0 GPa, i.e. a significant residual stress. The maxima of $-tE'$ disappear at higher temperatures. Only the left halves of the curves remain, and they are shifted towards lower $-tE'$ values and lower E values.

Calculated Kubát coefficients, K, are shown in Table 5. Values around those reported by Kubát (0.1) are obtained if E_0 is set to $E(t = 0.1$ s), and the extrapolation mentioned above is used to find E_∞ (K^* values in Table 5). On the other hand, with extrapolations for both E_0 and E_∞, lower K values are obtained (the lowest value corresponds to $\gamma = 0.16$). No consistent processing effect is observed if both K and K^* are

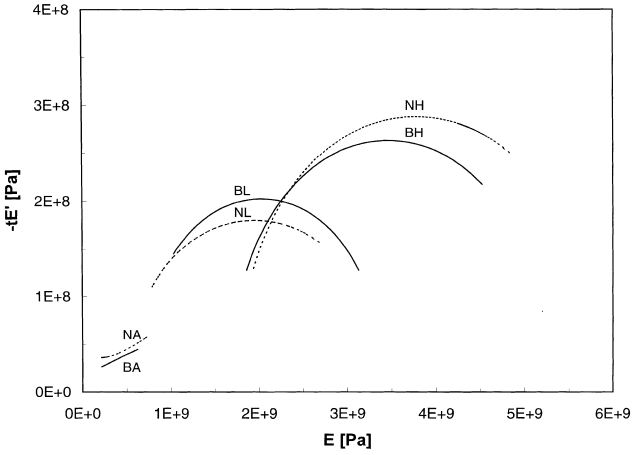

Fig. 9. $-tE'$ versus E at 23°C.

Table 5
Relaxation parameters obtained by extrapolation of $-tE'$ at 23°C (see text for details)

Sample	K	K^*[a]	$(E_0 - E_\infty)/E_0$
NH	0.071	0.096	0.70
BH	0.059	0.094	0.68
NL	0.068	0.085	0.85
BL	0.065	0.083	0.81

[a] The modulus at $t = 0.1$ s was used for E_0.

considered. In order to achieve better estimates for K, the total relaxation time should have been longer than in the present experiments. However, there seems to be a trend that the broad MWD gives lower coefficients, i.e. broader relaxations. It should be noted that Kubát, in his original paper [52], reported that K values for PP deviated from 0.1. This was attributed to internal stresses. Furthermore, the Kubát relation does not hold near thermal transitions [53].

The 'asymptotic' degree of relaxation can also be calculated with these extrapolations, as shown in the last column of Table 5. This value decreases with increasing draw ratio and polydispersity, which is consistent with values reported in Table 3, based on the relaxation during the time span of the experiment.

3.5. Time–temperature relationships

Semi-crystalline materials are generally not thermo-rheologically simple materials, i.e. a master curve—$E(t)$ at a certain reference temperature—cannot be constructed by only shifting data obtained at different temperatures along the time axis. Wortmann and Schultz recently addressed this issue for PP [12,13].

Although only a few temperatures were probed in the present study, horizontal shifts of data obtained for drawn fibres at 100 and 135°C do not contribute to realistic master curves. In particular, the stress plateaus do not comply with thermo-rheological simplicity. Attempts to construct master curves for $-tE'$ versus E (see Fig. 9) fail in a similar way.

Both viscoelastic and structural relaxation may occur in the fibres [22]. Examples of structural relaxation observed in PP are secondary crystallization [54] and physical ageing [28]. Different morphologies may be probed at different testing temperatures, due to structural reorganization. This may especially be a problem with highly oriented and quenched structures, i.e. structures far from equilibrium. The stress plateaus observed at 100°C may partly be induced by structural relaxation. (Their absence at 135°C may be due to 'thermal breakdown' of the anchoring elements.) The shrinkage observed in this study is a clear sign of structural relaxation. The α relaxation process is claimed to control the shrinkage of PP fibres [22]. Finally, it should be noted that if the equilibration time at an elevated temperature is too short, viscoelastic and structural relaxation will interfere.

4. Summary and conclusions

This study shows that the stress relaxation behaviour of polypropylene fibres is a function of molecular weight parameters and processing conditions. Both the average level of the relaxation curves and the relaxation kinetics are affected.

The wide range of relaxation responses observed is due to the variety of structures—on different length scales—that may develop as a function of material parameters and processing conditions, and their interaction. The differences in relaxation behaviour may be categorized as primary and secondary effects. The former are related to the value of the tensile modulus per se, while the latter are linked to the MWD and/or the morphology. The MWD effects are probably related to the high-molecular-weight tail of the distribution.

The primary effects are easy to understand, since the modulus—or molecular orientation—'determines' the starting point and the general level of the relaxation curve. Another 'modulus effect' is the general decrease in relaxation rate with increasing degree of orientation, due to lower mobility. These primary effects are mainly related to processing conditions, via structural characteristics. At 23°C, the relaxation behaviour of the fibres is dominated by primary effects. Somewhat higher relaxation rates for fibres with a narrow MWD are also observed, in accordance with reptation theory. A higher degree of structural homogeneity in these fibres may also play a role.

At 100°C, MWD effects are more pronounced, but only for drawn fibres with α-crystalline structure. Higher temperatures correspond to longer relaxation times and larger length scales. Hence, the focus is shifted towards the reptation of long chain segments, including 'anchorage' effects. Higher initial values for stresses and relaxation rates, observed for fibres with a broad MWD, can be understood by considering the DMTA data: In an intermediate temperature interval, ending somewhat below 100°C, fibres with a narrow MWD have higher 'relaxation strength' than those with a broad MWD. At higher temperatures, this relationship is reversed. The same DMTA trends are observed for as-spun (mesomorphic) fibres, but the stress relaxation is not influenced in the same way as for drawn fibres. Hence, the relaxation of fibres with a broad MWD seems to be delayed, but not by a purely viscoelastic effect; the presence of crystalline regions, or the interphase between crystalline and amorphous regions, plays a decisive role.

Another MWD effect is observed at 100°C, namely a stress plateau at long relaxation times for crystalline fibres with a broad MWD. As this effect is not observed by DMTA, the plateaus may be due to physical cross-links at crystalline entities that developed during the stress relaxation experiment.

In addition to classical linear viscoelastic relaxation, specialized mechanical models should account for non-linearity and structural relaxation, including effects induced by molecular weight parameters and processing conditions, such as those presented in this article. Furthermore, a good theory for the mechanical response should cover all relevant stress distributions and loading histories. As an example [2,55], a constitutive equation applied to uniaxial tension should predict tensile moduli versus time obtained with constant strain (stress relaxation), constant stress (creep) and constant strain rate (conventional tensile testing).

Acknowledgements

This work was supported by Borealis AS and the Research Council of Norway. The author is indebted to Ole Jan Myhre (Borealis AS) for initializing a project on PP fibres some years ago, and for providing the samples. Einar L. Hinrichsen (SINTEF) is gratefully acknowledged for critically reviewing the manuscript.

References

[1] Ward IM, Hadley DW. An introduction to the mechanical properties of solid polymers. Chichester: Wiley, 1993.
[2] Matsuoka M. Relaxation phenomena in polymers. Munich: Hanser, 1992.
[3] Ferry JD. Viscoelastic properties of polymers, 3rd edn. New York: Wiley, 1980.
[4] Boyd RH. Polymer 1985;26:323.
[5] Boyd RH. Polymer 1985;26:1123.
[6] McCrum NG. Polymer 1984;25:299.
[7] Read BE. Polymer 1989;30:1439.
[8] Rutledge GC, Suter UW. Macromolecules 1992;25:1546.
[9] Jourdan C, Cavaille JY, Perez J. J Polym Sci Polym Phys Ed 1989;27:2361.
[10] Wool RP, Statton WO. J Polym Sci Polym Phys Ed 1974;12:1575.
[11] Wortmann F-J, Schultz KV. Polymer 1995;36:315.
[12] Wortmann F-J, Schultz KV. Polymer 1995;36:1611.
[13] Wortmann F-J, Schultz KV. Polymer 1996;37:819.
[14] Wortmann F-J, Schultz KV. Polymer 1994;35:2108.
[15] Wortmann F-J, Schultz KV. Polymer 1995;36:2363.
[16] Dutta NK, Edward GH. J Appl Polym Sci 1997;66:1101.
[17] Ariyama T, Mori Y, Kaneko K. Polym Eng Sci 1997;37:81.
[18] Ariyama T. J Mater Sci 1996;31:4127.
[19] Ariyama T. Polym Eng Sci 1995;35:1455.
[20] Ariyama T. Polym Eng Sci 1993;33:1494.
[21] Gol'dman AYa. Prediction of the deformation properties of polymeric and composite materials. Washington, DC: ACS, 1994.
[22] Bhuvanesh YC, Gupta VB. Polymer 1995;36:3669.
[23] Tomlins PE, Read BE. Polymer 1998;39:355.
[24] Read BE, Tomlins PE. Polym Eng Sci 1997;37:1572.
[25] Read BE, Tomlins PE. Polymer 1997;38:4617.
[26] Hellinckx S. Colloid Polym Sci 1995;273:130.
[27] Hutchinson JM, Kriesten U. J Non-Cryst Solids 1994:172–174, 592.
[28] Buckley CP, Habibullah M. J Appl Polym Sci 1981;26:2613.
[29] Teoh SH, Poo AN, Ong GB. J Mater Sci 1994;29:4918.
[30] Attalla G, Guanella IB, Cohen RE. Polym Eng Sci 1983;23:883.
[31] Passaglia E, Martin GM. J Research Nat Bur Stand—A Phys Chem 1964;68A:519.
[32] Kawamoto N, Mori H, Yui N, Nitta KH, Terano M. Angew Makromol Chem 1996;243:87.
[33] Crissman JM. J Polym Sci Part A-2 1969;7:389.
[34] De Candia F, Romano G, Baranov AO, Prut EV. J Appl Polym Sci 1992;46:1799.

[35] Jawad SA, Alhaj-Mohammad MH. Polym Int 1994;35:395.
[36] Sawatari C, Matsuo M. Macromolecules 1989;22:2968.
[37] Hadley DW, Ward IM. J Mech Phys Solids 1965;13:397.
[38] Flocke HA. Koll-Z, Z Polym 1962;180:118.
[39] Deiber JA, Peirotti MB, Gappa A. J Elast Plast 1997;29:290.
[40] Sakata Y, Unwin AP, Ward IM. J Mater Sci 1995;30:5841.
[41] Andreassen E, Myhre OJ, Hinrichsen EL, Grøstad K. J Appl Polym Sci 1994;52:1505.
[42] Andreassen E, Hinrichsen EL, Grøstad K, Myhre OJ, Braathen MD. Polymer 1995;36:1189.
[43] Andreassen E, Myhre OJ, Oldervoll F, Hinrichsen EL, Grøstad K, Braathen MD. J Appl Polym Sci 1995;58:1619.
[44] Andreassen E, Gundersen E, Hinrichsen EL, Langtangen HP. In: Dæhlen M, Tveito A, editors. Numerical methods and software tools in industrial mathematics. Boston, Ma: Birkhäuser, 1997:195–212.
[45] Andreassen E, Myhre OJ. J Appl Polym Sci 1993;50:1715.
[46] Andreassen E, Grøstad K, Myhre OJ, Braathen MD, Hinrichsen EL, Syre AMV, Løvgren TB. J Appl Polym Sci 1995;57:1075.
[47] Andreassen E, Myhre OJ, Hinrichsen EL, Braathen MD, Grøstad K. J Appl Polym Sci 1995;58:1633.
[48] Foreman JA, Klinger KA, Wolkowicz M. Thermochim Acta 1996;272:147.
[49] Knoff WF, Hopkins IL, Tobolsky AV. Macromolecules 1971;4:750.
[50] Santangelo PG, Ngai KL, Roland CM. Polymer 1998;39:681.
[51] Brostow W, Kubát J, Kubát M. J Mech Compos Mater 1995;31:432.
[52] Kubát J. Nature 1965;205:378.
[53] Kubát DG, Bertilsson H, Kubát J, Uggla S. J Phys: Condens Matter 1992;4:7041.
[54] Albrecht T, Strobl G. Macromolecules 1995;28:5267.
[55] Kontou E. J Appl Polym Sci 1998;67:679.